

See discussions, stats, and author profiles for this publication at: <https://www.researchgate.net/publication/343520704>

# Detection Of Skin Cancer Using Deep Neural Networks

Conference Paper · December 2019

DOI: 10.1109/CSD48274.2019.9162400

CITATIONS

27

READS

1,368

6 authors, including:



**Muzahidul Rahi**  
BRAC University

8 PUBLICATIONS 65 CITATIONS

SEE PROFILE



**Farhan Tanvir Khan**

3 PUBLICATIONS 33 CITATIONS

SEE PROFILE



**Mohammad Tanvir Mahtab**  
BRAC University

5 PUBLICATIONS 39 CITATIONS

SEE PROFILE



**A. K. M. Amanat Ullah**  
University of British Columbia - Okanagan

14 PUBLICATIONS 51 CITATIONS

SEE PROFILE

# DETECTION OF SKIN CANCER USING DEEP NEURAL NETWORKS

Md. Muzahidul Islam Rahi  
Department of Computer Science and  
Engineering  
BRAC University  
Dhaka, Bangladesh  
md.muzahidul.islam.rahi@g.bracu.ac.bd

Farhan Tanvir Khan  
Department of Computer Science and  
Engineering  
BRAC University  
Dhaka, Bangladesh  
farhan.tanvir.khan@g.bracu.ac.bd

Mohammad Tanvir Mahtab  
Department of Computer Science and  
Engineering  
BRAC University  
Dhaka, Bangladesh  
mohammad.tanvir.mahtab@g.bracu.ac.bd

A. K. M. Amanat Ullah  
Department of Computer Science and  
Engineering  
BRAC University  
Dhaka, Bangladesh  
a.k.m.amanat.ullah@g.bracu.ac.bd

Md. Golam Rabiul Alam  
Department of Computer Science and  
Engineering  
BRAC University  
Dhaka, Bangladesh  
rabiul.alam@bracu.ac.bd

Md. Ashraful Alam  
Department of Computer Science and  
Engineering  
BRAC University  
Dhaka, Bangladesh  
ashraful.alam@bracu.ac.bd

**Abstract**—Skin cancer is a huge issue which gets neglected very often. Sometimes the human eye is unable to precisely detect diseases from imaging data, in cases of doctor's manual inspection. In this age, we see the rise of use of deep learning methods in our daily life problem solving. Therefore, we develop an automated computerised system for detecting skin diseases using deep neural network algorithms. In the proposed model, we have used several neural network algorithms and analyse their performances to detect five major skin diseases and figure out the best performing algorithm in terms of accuracy. CNN and by using Keras Sequential API, we have structured a new model to gain an accuracy of around 80%. Later, for comparison and also to increase accuracy we have used architectures that use pre-trained data. These transfer learning model includes VGG11, RESNET50 and DENSENET121. Among the algorithms used in the proposed models, resnet architecture achieve highest accuracy of 90%.

**Keywords**—neural network; machine learning; deep learning; transfer learning; pretrained data

## I. INTRODUCTION

In the world around us we see people suffering from skin diseases but they seem to overlook thinking it might be just like any typical skin disease they might suffer from. But little do they know how dangerous this might get if they don't know what they are actually suffering from and take necessary precautions by going to the right doctor and get prescribed with proper medication. We know how people who live in the rural areas of underdeveloped countries or developing countries such as Bangladesh, Sri Lanka, India etc. have so little or no access to doctors and let alone be doctors who are skin specialists. Our main motivation was to help people identify these diseases at their early stage as most of the types people ignore skin lesions. Even human eyes does not have enough accuracy and that also goes for doctors. Our objective is to use modern technological advances in the realms of medical science and also use our knowledge of neural network to help ease a problem. With the help of our knowledge from

our institution and the dataset that is collected from ISIC archive, we desire to build a system for helping skin cancer patients. According to Oxford Journals, there are 1.3 to 1.5 million disease patients in Bangladesh, with around 0.2 million patients recently determined to have malignancy every year. So when people like these have any skin disease, either they choose to avoid it or when they realize it's high time to consult a proper doctor, it's too late. Also Doctors at those areas are not usually experts to understand skin diseases that can cause cancers. Even in a place like U.S where you have the best hospitals equipped with the best of the best doctors, still the rate of death because of cancer still very high. If more people could have gotten more precocious from an earlier time then they would have known that it's not any typical skin lesion, rather something life threatening. This is where our model of detecting skin cancer from mere images comes in. Our model will process the images and by the help of the algorithm used, it will detect the probability of that skin disease of being cancerous[24].

We have gone through several papers which aided us in doing our thesis work. They gave us the idea, motivation and guided us in difficult times. Our work focuses on detection of skin cancer using different neural networks so we looked into several methods which use neural networks and machine learning to try to solve the same problem. One of the major works in this field was "Automatic Detection of Melanoma Skin Cancer using Texture Analysis" by Mariam A. Sheha, Cairo University. This paper aims to detect Melanoma which is a skin related cancer and it is life-threatening. In the USA in the year 2011, around 70 thousand people were diagnosed with melanoma and around 9 thousand people died because of the disease in the same year[25]. They have distinguished between melanocytic nevi and malignant melanoma using texture analysis in their system[19]. PC is not wiser than human yet it might almost certainly remove some data, for example, surface highlights,

that may not be promptly seen by human eyes. A few scoring frameworks and calculations, for example, the ABCD rule for epiluminescence, the seven-point agenda, and the Menzies technique [11][18]. A large portion of the proposed procedures require division process that considers being a lethal issue because of the abnormality of the tumor, where dermoscopy perspectives on histological tissues show structures for the most part organized in an assortment of examples. So that, programmed division of various structures, similar to cores, cytoplasm, vessels and so on., is troublesome, and is impossible when all is said in done approach [9][1][14][4][16]. As of late, PC supported dermoscopy utilizing fake neural systems (ANNs) has been accounted for to be a precise apparatus for the assessment of pigmented skin sores (PSLs) [12][20][21]. The Artificial Neural Network they applied is MLP and represent the classes of the 2 diseases, whereas we used different neural networks such as ResNet, DenseNet and VGG models to classify 7 types of skin lesions. They have used 2 types of MLP: Automatic and Traditional. The authors have also addressed previous related work in achieving their goals. They have referred to various kinds of ways proposed that were used to improve accuracy of diagnosis. ELM (Epiluminescence Microscopy) described in 1987 and it uses incident light, oil immersion and magnifier. TCA (Tissue Counter Analysis), which uses image partition into equal squares from which features are calculated [22].

Advancement of non-obtrusive instruments to improve early conclusion brings about 2 approaches, dermoscopy and computerized picture investigation [21]. Picture chart books of reference pictures are generally accessible [23]. Classification is based on co-occurrence matrix texture features to distinguish between melanocytic nevi and melanoma. MLP (Multilayer Perceptron) generates nonlinear boundaries and is a feed forward network [6][15][17]. They have divided data into the following proportions: 60% to train, 20% to test and 20% for validation. In contrast to our own work which is 80% training and 20% testing and then a further 20% from the train data for validation purposes. The results of this paper is given in Figure 2.2. Another work which we studied was "Neural Network Diagnosis of Malignant Melanoma from Color Images" by Fikret Ercal, Senior Member, IEEE Anurag Chawla [13]. In this paper, the authors talked about using colored images of skin lesions combined with image processing techniques and an ANN (Artificial Neural Network) to separate melanoma from 3 other tumours: dysplastic nevi, intradermal nevi and seborrheic keratoses. To do this they used a feedforward artificial neural network with 14 inputs and 1 output stating whether or not the tumor is melanoma. This model was used and trained by backpropagation rule. They also said that they used NeuralWorks which is a commercial neural network software. As of late, neural systems have been utilized as pattern classifiers in restorative analysis [8], [7], discourse [3] and pattern acknowledgment [2], and computerized reasoning applications. Indicative applications require a choice of highlights that must be customized

independently for every issue space. The features chosen ought to contain enough data to recognize classes while being heartless toward immaterial inconstancy in the information sources. They characterized 14 highlights that we accept to be well discriminative between pictures having a place with harmful melanoma. The majority of the 14 highlights that were distinguished to be helpful in finding required discovery of the outskirts of the tumor in the shading picture. Limit recognition is clarified in detail by Golston et al. [5] and Ercal et al. [10].

## II. METHODOLOGY

At first we ran our own CNN model shown in Figure 1, on the dataset (HAM10000) we got from ISIC archive. Later to get better and more accurate results, we used VGG, ResNet and DenseNet methods. These allow rapid progress or improved performance when modelling the second task to increase our accuracy.

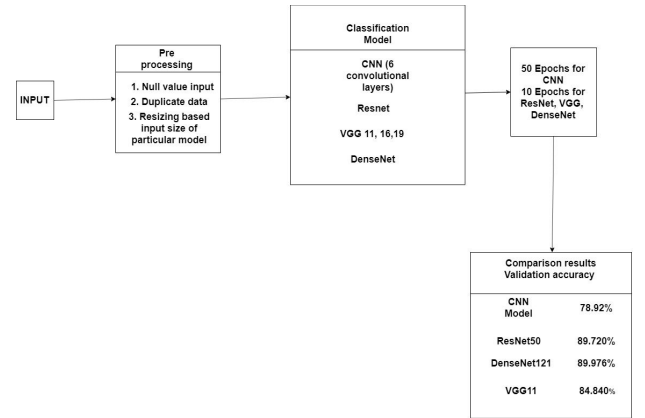


Figure 1: Our Proposed model

## III. MODEL TRAINING

### A. Loading and resizing of images

In this step images will be loaded into the column named image from the image path from the image folder. We also resize the images as the original dimension of images are 450 x 600 x 3 which TensorFlow can not handle, so that's why we resize it into 100 x 75 x 3.

### B. Test-Train Split

We have split the dataset into testing and training set of 80:20 ratio.

### C. Normalization

We normalized train set and test set by subtracting from their mean values and then dividing by their standard deviation. This is normalize all values from 0- 255 to 0-1.

### D. Label Encoding

Labels are 7 different classes of skin cancer types from 0 to 6. The labels are Actinic keratoses, Basal cell carcinoma, Benign keratosis-like lesions,

Dermatofibroma, Melanoma, Melanocytic nevi and Vascular lesions

#### E. Splitting training and validation split

We took 90% of the data to train our model. 10% of the data was used to test our model. a small test or validation dataset is used here to minimize overfitting.

#### F. Data Augmentation

For our model we rotated the sample images by 10 degrees zoomed in by 10%. the images were also shifted 10% both horizontally and vertically to further increase the size of our training sample.

### IV. MODEL IMPLEMENTATION

We used the Keras Sequential API. The initial step is the convolutional layers which are basically a set of filters to learn features from the images. 128 filters are chosen for the two layers followed by four conv2D layers each with 64 filters. The filters are called Kernel filters and they perform transformation of the images. The filters are 2D matrix and are applied on all the images. The CNN can separate features from these images which are necessary for the classification task. After that we have pooling (MaxPool2D) layer. This layer works as a downsampling filter. It picks the maximum value from the two neighbouring pixels. We use this to minimize computational cost and also in cases of reducing overfitting, this can be used. For this to work we need to work, we need to set the pooling size and if the size is higher, necessarily downsampling becomes more important. By incorporating Conv2D and Pooling layers both global and local features are learned. As to select the training sample, some part of the nodes in this layer have their weights set to 0. This is known as Dropout and it is a regularization method. A percentage of the network is dropped and forces the system to learn features in a distributed way. This normalization is improved and overfitting is reduced. We have used 'Relu' which is a rectifier. The activation function is given by  $\max(0, x)$  and it adds non linearity to the system. Next the final feature map is converted into an only 1D vector in the Flattening Layer. Flattening is required after convolution and max pooling to use the fully connected layers. It brings together the local features from the earlier convolutional layers. Figure below shows 1D vector as the input layer. Finally, the features of 2 fully connected, Dense layers, which are fundamentally ANN (Artificial Neural Networks) classifiers. The net outputs distribution of probability of every class can be found in the final layer, where the net outputs distribution of probability of each class. The diagram above shows 1D vector as the input layer. The Figure below shows 1D vector as the input layer.

Layer (type)	Output Shape	Param #
conv2d_1 (Conv2D)	(None, 75, 100, 128)	3584
conv2d_2 (Conv2D)	(None, 75, 100, 128)	147584
max_pooling2d_1 (MaxPooling2D)	(None, 37, 50, 128)	0
dropout_1 (Dropout)	(None, 37, 50, 128)	0
conv2d_3 (Conv2D)	(None, 37, 50, 64)	73792
conv2d_4 (Conv2D)	(None, 37, 50, 64)	36928
max_pooling2d_2 (MaxPooling2D)	(None, 18, 25, 64)	0
dropout_2 (Dropout)	(None, 18, 25, 64)	0
conv2d_5 (Conv2D)	(None, 18, 25, 64)	36928
conv2d_6 (Conv2D)	(None, 18, 25, 64)	36928
max_pooling2d_3 (MaxPooling2D)	(None, 9, 12, 64)	0
dropout_3 (Dropout)	(None, 9, 12, 64)	0
flatten_1 (Flatten)	(None, 6912)	0
dense_1 (Dense)	(None, 128)	884864
dropout_4 (Dropout)	(None, 128)	0
dense_2 (Dense)	(None, 7)	983
Total params: 1,221,511		
Trainable params: 1,221,511		
Non-trainable params: 0		

Figure 2: The Architecture of our Model

For the models we used ADAM optimizer. The algorithm which was mentioned before expands stochastic gradient descent which was used in wider adaptation of deep learning implementation in computer vision in both computer vision and natural learning processing. By this method, the parameters are made much better by repeatedly going through the kernel values, at the same time the weights and also bias of neurons thus reducing the percentage loss. Later when the layers were joined, a few functions were set up which included a score function, a loss function and finally a tuning algorithm. The performance on the pictures with the known features or the labels were measured by the loss function which assessed how poorly the model performed. So this is the rate of error between the perceived label and the forecasted error. A specific type of categorical classification is used called categorical cross entropy with the optimizer being the most important function and it will improve parameters iteratively to minimize loss.

For making the optimizer converge quicker and as close to as low as possible, an annealing function of learning rate (LR) is used. The LR is the process where the optimizer explores the "loss region". A high LR means that the steps are large and convergence occurs faster, although, the sampling is quite poor and the optimizer is prone to be in the local minima. A better proposition is to have a reduced LR while in the training stage to get to the lowest loss function efficiently. But the fast computation time of high LR is advantageous and keeping that benefit is desirable, thus LR was reduced dynamically in every epoch where required when accuracy did not improve. ReduceLROnPlateau

function from Keras.callbacks was used to decrease the LR by half when accuracy did not increase after 3 epochs. Batch size of 10 and 50 epochs was chosen and the model was trained into x train and y train. A small batch size of 10 made training more efficient and 50 epochs on the other hand was large enough to train the model in the first place. Later to improve the accuracy to increase the accuracy, we have used ResNet50, DenseNet121 and VGG11 Batch Normalization (BN). Trained on over 1 million pictures from ImageNet, this network consists of 50 layers. Images can be grouped into 1000 object categories. This network is capable of working on a wide range of images due to its rich network. Whereas plain networks are stacked one over the other, residual networks utilize skip-connections as shortcuts to jump over some layers. ResNet models are integrated with double or even triple layer skips that contain non-linearities (ReLU) and in between there are batch normalizations. Skipping over layers are done so that vanishing gradient problem can be avoided. This is done by reusing the activations from a previous layer until the adjacent layers know its weight. Jumping over layers therefore simplifies the network and uses less number of layers during the training stage. The network has an image input size of 224 x 224 x 3. The figure shows the algorithm of ResNet.

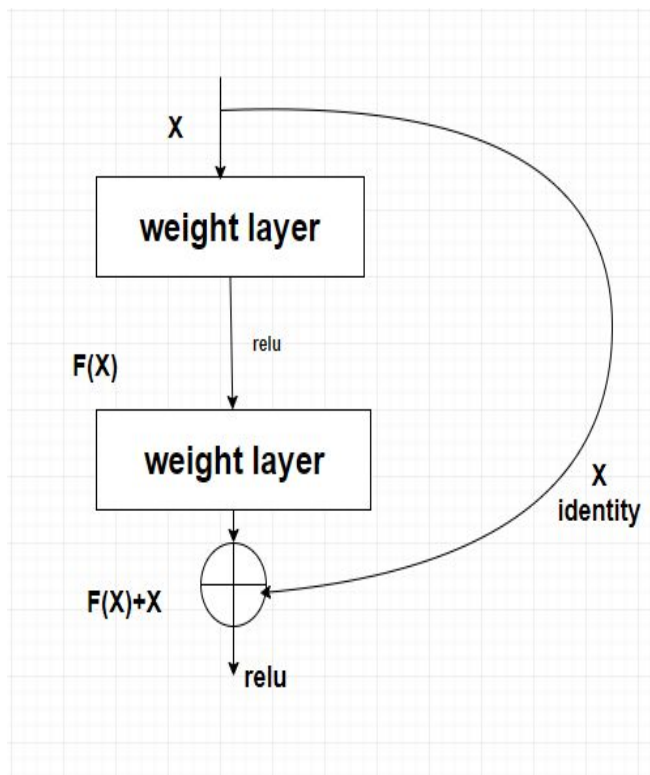


Figure 3: ResNet50 Algorithm

DenseNets simplify connectivity pattern between layers in the other architectures such as Residual Networks. DenseNets take advantage of potential of the network by reusing feature. Every layer is connected with each other. Due to this connection, DenseNets need less parameters than traditional CNN because the need to learn redundant feature maps is eliminated. It is proven that in some types of

ResNets, not all layers are useful and they can simply be dropped. ResNets are huge with every layer having its own learned weights. To counter this, DenseNets use narrow layers with the addition of smaller sets of new feature-maps. Additionally, DenseNets have every layer with access to the gradients from the loss function and the original input image which helps solve the problem during training stage with information flow and gradients. DenseNets avoid summing the output feature maps of the layer with incoming 36 feature maps. Instead they concatenate. DenseNets are divided into DenseBlocks where the feature maps remain the same in size and dimensions but the amount of filters applied changes in between. The in-between layers are called Transition Layers and handle downsampling by batch normalization, one 1x1 convolution and 2x2 pooling layers.

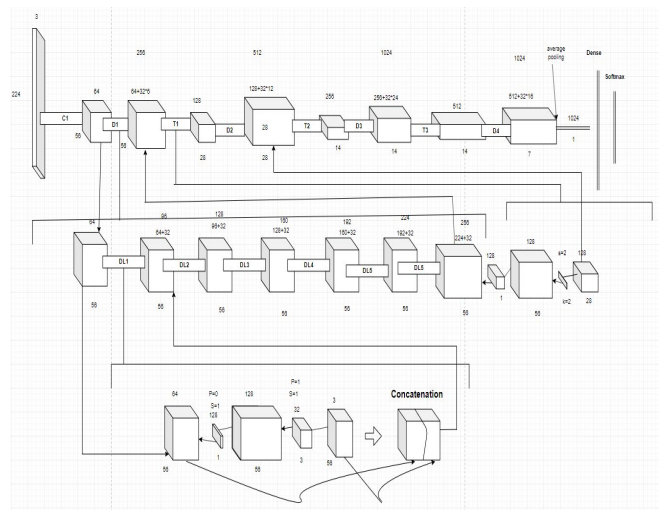


Figure 4: Full schematic representation of DenseNet121

In Figure 4, every layer is adding to preceding volume 32 feature maps. For this reason, it goes from 64 to 256 after 6 whole layers. Transition Block works as 1x1 convolution with 128 filters then a 2x2 pooling with 2 strides. This results in volume and feature maps to be halved after every Transition block. After this we can perform a more expensive 3x3 convolution with the chosen 32 feature maps of growth rate. Then, the input volume and output of the 2 operations are concatenated. This adds new information to the shared knowledge of the network.

Next we have used VGG11 in our proposed model. VGG11 already obtains 10.4% error rate. VGG uses pre trained data to increase accuracy. VGG11 has 133 million parameters whereas VGG16 has 138 million and VGG19 has 144 million parameters. VGG11 is the predecessor to VGG16 and VGG19. The figure shows the architecture of all the VGG models. Surprisingly, using VGG16 and VGG19, we failed to get a desired outcome with 10 epochs. Both models showed similar outcomes, so we showed the last two epochs out of the ten. Both the epoch shows high irregularity in validation accuracies and the failure in having reasonable training accuracy leads to under-fitting. As a solution to this, we chose to apply our model using VGG11 BN (Batch Normalization).



ConvNet Configuration					
A	A-LRN	B	C	D	E
11 weight layers	11 weight layers	13 weight layers	16 weight layers	16 weight layers	19 weight layers
input(224x224 RGB image)					
conv3-64	conv3-64 LRN	conv3-64 conv3-64	conv3-64 conv3-64	conv3-64 conv3-64	conv3-64 conv3-64
maxpool					
conv3-128	conv3-128	conv3-128 conv3-128	conv3-128 conv3-128	conv3-128 conv3-128	conv3-128 conv3-128
maxpool					
conv3-256 conv3-256	conv3-256 conv3-256	conv3-256 conv3-256	conv3-256 conv3-256 conv3-256	conv3-256 conv3-256 conv3-256	conv3-256 conv3-256 conv3-256
maxpool					
conv3-512 conv3-512	conv3-512 conv3-512	conv3-512 conv3-512	conv3-512 conv3-512 conv3-512	conv3-512 conv3-512 conv3-512	conv3-512 conv3-512 conv3-512
maxpool					
conv3-512 conv3-512	conv3-512 conv3-512	conv3-512 conv3-512	conv3-512 conv3-512 conv3-512	conv3-512 conv3-512 conv3-512	conv3-512 conv3-512 conv3-512
maxpool					
FC-4096					
FC-4096					
FC-1000					
soft-max					

Figure 5: Architecture of VGG Models

## V. MODEL EVALUATION

	CNN Model	ResNet50	DenseNet 121	VGG11 BN
Validation Accuracy	79%	90%	90%	85%

Table 1: Validation Accuracy for our model

As we can see from Table 1, the results from all the models we have used. Overall ResNet50 consistently produced around 90% accuracy. For ResNet50, DenseNet 121 and VGG11 we have used 10 epochs and for our CNN model, we have used 50 epochs. Given that ResNet50 showed consistent accurate results we implemented this model to evaluate our system.

```
[epoch 10], [iter 100 / 1124], [train loss 0.25444], [train acc 0.90031]
[epoch 10], [iter 200 / 1124], [train loss 0.25240], [train acc 0.90422]
[epoch 10], [iter 300 / 1124], [train loss 0.26108], [train acc 0.89979]
[epoch 10], [iter 400 / 1124], [train loss 0.25361], [train acc 0.90312]
[epoch 10], [iter 500 / 1124], [train loss 0.25032], [train acc 0.90500]
[epoch 10], [iter 600 / 1124], [train loss 0.25092], [train acc 0.90484]
[epoch 10], [iter 700 / 1124], [train loss 0.25462], [train acc 0.90237]
[epoch 10], [iter 800 / 1124], [train loss 0.25331], [train acc 0.90285]
[epoch 10], [iter 900 / 1124], [train loss 0.25478], [train acc 0.90201]
[epoch 10], [iter 1000 / 1124], [train loss 0.25308], [train acc 0.90303]
[epoch 10], [iter 1100 / 1124], [train loss 0.25251], [train acc 0.90347]

-----
[epoch 10], [val loss 0.33129], [val acc 0.89720]
-----

*****
best record: [epoch 10], [val loss 0.33129], [val acc 0.89720]
*****
```

Figure 6: Validation Accuracy for the last epoch for ResNet50

The graph in Figure 7 shows, Validation loss and Validation accuracy for ResNet50.

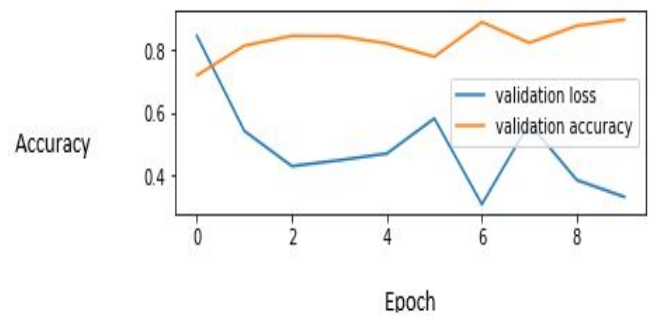


Figure 7: Validation loss and Validation accuracy for ResNet50

The graph in Figure 8 shows, Training loss and Training accuracy for ResNet50.

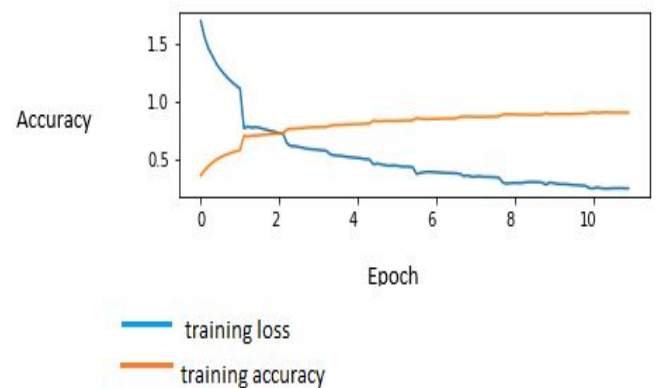


Figure 8: Training loss and Training accuracy for ResNet50

A confusion matrix is a tabular design that allows understanding of the calculation, how much of it is predicting correctly. It is a special sort of probability table, with 2 measurements ("true" and "predicted"), and inseparable sorting of "labels" in the two measurements. Figure 9, shows the confusion matrix for ResNet50.

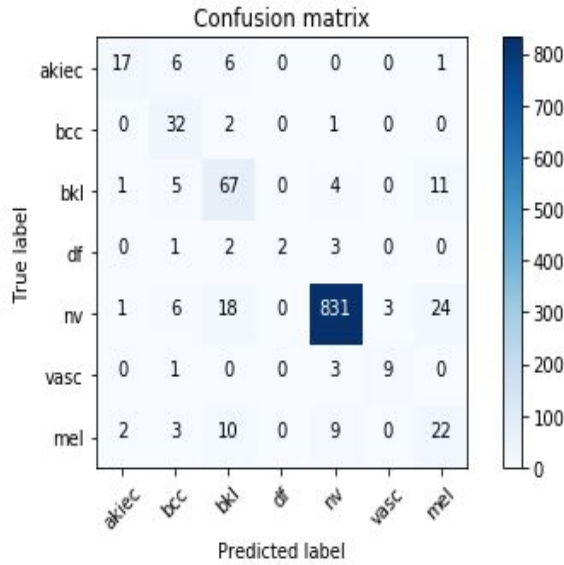


Figure 9: Confusion matrix for CNN

These graphs tell us the percentage of wrongly classified data. This is shown in the figure below for ResNet50.

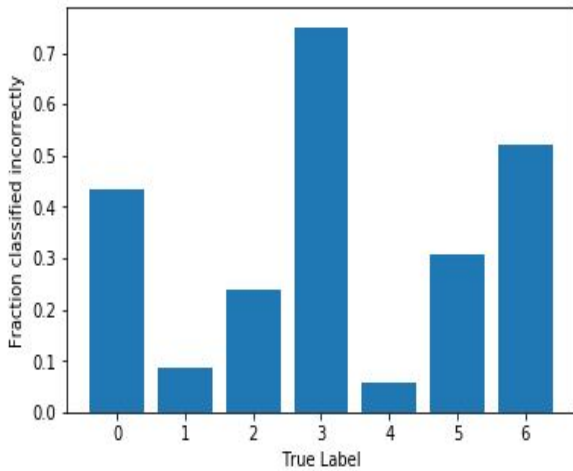


Figure 10: Fraction classified incorrectly for ResNet50

These are methods to evaluate our system. We cannot just determine a system by accuracy only. To understand precision, recall, f1 score or support, we need to first understand the concept of True Negative, False Negative, True Positive and True Negative. The Table 2 shows, the concept of these.

		Predicted	
		Negative	Positive
Actual	Negative	True Negative	False Positive
	Positive	False Negative	True Positive

Table 2: True Negative, False Negative, True Positive and True Negative description

**Precision** - Calculates relevant instances out of retrieved instances.

$$\text{Precision} = \text{True Positive} / (\text{True Positive} + \text{False Positive})$$

**Recall** - Calculates the number of true positives among the total number of true positives.

$$\text{Recall} = \text{True Positive} / (\text{True Positive} + \text{False Negative})$$

**F1 Score** - This is the balance between Precision and Recall. This is a better measure of test accuracy.

$$\text{F1 Score} = 2 * (\text{Precision} * \text{Recall}) / (\text{Precision} + \text{Recall})$$

**Support** - The support is the quantity of tests of the genuine reaction that lie in that class.

	precision	recall	f1-score	support
akiec	0.81	0.57	0.67	30
bcc	0.59	0.91	0.72	35
bkl	0.64	0.76	0.69	88
df	1.00	0.25	0.40	8
nv	0.98	0.94	0.96	883
vasc	0.75	0.69	0.72	13
mel	0.38	0.48	0.42	46
accuracy			0.89	1103
macro avg	0.74	0.66	0.65	1103
weighted avg	0.91	0.89	0.89	1103

Figure 11: Precision, Recall, F1 score and Support for ResNet50

Figure 11 shows, the precision, recall, F1 score and support for ResNet50 after 10 epochs.

## VI. CONCLUSION

This paper discusses about the concept about identifying different types of skin cancer using a CNN model by Keras Sequential API. We have set our kernel size for our convolution and filter size for our max-pooling. We finally flattened these into 1D single vector and then into the ANN from Keras. Our database consisted of 10015 images and we split it into 80:20 for test and train. We further split the train set into 10% validation. Using our 6 layered CNN model, we were getting around 79% accuracy in training with the validation set and around 76% using the test set where we ran our model for 50 epochs. We wanted to increase the accuracy and thus we used CNN algorithm on VGG11, ResNet50 and DenseNet121 models, which uses pre-trained data from ImageNet. These models increased the magnitude of our dataset and thus increases our

efficiency of the model. Using these we were able to reach 90% accuracy in training and minimal amount of loss. For all of these models, we used 10 epochs and for evaluation we drew graphs of loss and accuracy, confusion matrix, incorrect predictions and so on. We also calculated precision, support, F1 score and recall. We believe that a system which is able to detect 90% accurately just with the image can work in areas where this model is efficient in comparison to detection with human eyes. Our future plan is to use our models for detecting skin cancer in a real life settings so that people who have little facility of receiving medical help, can benefit from our project.

## REFERENCES

- [1] H. Harms, H. Aus, M. Haucke, and U. Gunzer, "Segmentation of stained blood cell images measured at high scanning density with high magnification and high numerical aperture optics," *Cytometry: The Journal of the International Society for Analytical Cytology*, vol. 7, no. 6, pp. 522–531, 1986.
- [2] T. Kohonen, G. Barna, and R. Chrisley, "Statistical pattern recognition with neural networks: Benchmarking studies", in *IEEE International Conference On Neural Networks*, vol. 1, 1988, pp. 61–68.
- [3] R. P. Lippmann, "Review of neural networks for speech recognition," *Neural computation*, vol. 1, no. 1, pp. 1–38, 1989.
- [4] A. R. Brown, "Combined immunocytochemical staining and image analysis for the study of lymphocyte specificity and function in situ", *Journal of immunological methods*, vol. 130, no. 1, pp. 111–121, 1990.
- [5] J. E. Golston, R. H. Moss, and W. V. Stoecker, "Boundary detection in skin tumor images: An overall approach and a radial search algorithm", *Pattern Recognition*, vol. 23, no. 11, pp. 1235–1247, 1990.
- [6] J. A. Freeman and D. M. Skapura, *Neural networks: algorithms, applications, and programming techniques*. Addison Wesley Longman Publishing Co., Inc., 1991.
- [7] R. Poli, S. Cagnoni, R. Livi, G. Coppini, and G. Valli, "A neural network expert system for diagnosing and treating hypertension", *Computer*, vol. 24, no. 3, pp. 64–71, 1991.
- [8] M. L. Astion and P. Wilding, "Application of neural networks to the interpretation of laboratory data in cancer diagnosis", *Clinical Chemistry*, vol. 38, no. 1, pp. 34–38, 1992.
- [9] T. W. McGOVERN and M. S. Litaker, "Clinical predictors of malignant pigmented lesions: A comparison of the glasgow seven-point checklist and the american Cancer society's abcds of pigmented lesions", *The Journal of dermatologic surgery and oncology*, vol. 18, no. 1, pp. 22–26, 1992.
- [10] F. Ercal, M. Moganti, W. Stoecker, and R. H. Moss, "Boundary detection and color segmentation in skin tumor images", in *Biomedical image processing and biomedical visualization*, International Society for Optics and Photonics, vol. 1905, 1993, pp. 900–910.
- [11] H. Pehamberger, M. Binder, A. Steiner, and K. Wolff, "In vivo epiluminescence microscopy: Improvement of early diagnosis of melanoma", *Journal of Investigative Dermatology*, vol. 100, no. 3, pp. S356–S362, 1993.
- [12] M. Binder, A. Steiner, M. Schwarz, S. Knollmayer, K. Wolff, and H. Pehamberger, "Application of an artificial neural network in epiluminescence microscopy pattern analysis of pigmented skin lesions: A pilot study", *British Journal of Dermatology*, vol. 130, no. 4, pp. 460–465, 1994.
- [13] F. Ercal, A. Chawla, W. V. Stoecker, H.-C. Lee, and R. H. Moss, "Neural network diagnosis of malignant melanoma from color images", *IEEE Transactions on biomedical engineering*, vol. 41, no. 9, pp. 837–845, 1994.
- [14] W. Stolz, T. Vogt, M. Landthaler, S. Hempfer, P. Bingler, and W. Abmayr, "Differentiation between malignant melanomas and benign melanocytic nevi by computerized DNA cytometry of imprint specimens", *Journal of cutaneous pathology*, vol. 21, no. 1, pp. 7–15, 1994.
- [15] C. M. Bishop et al., *Neural networks for pattern recognition*. Oxford university press, 1995.
- [16] P. W. Hamilton, P. H. Bartels, R. Montironi, N. H. Anderson, D. Thompson, J. Diamond, S. Trewin, and H. Bharucha, "Automated histometry in quantitative prostate pathology", *Analytical and quantitative cytology and histology*, vol. 20, no. 5, pp. 443–460, 1998.
- [17] M. Kubat, "Neural networks: A comprehensive foundation by simon haykin", *macmillan*, 1994, isbn 0-02-352781-7. *The Knowledge Engineering Review*, vol. 13, no. 4, pp. 409–412, 1999.
- [18] M.-L. Bafounta, A. Beauchet, P. Aegerter, and P. Saiag, "Is dermoscopy (epi-luminescence microscopy) useful for the diagnosis of melanoma?: Results of a meta-analysis using techniques adapted to the evaluation of diagnostic tests", *Archives of dermatology*, vol. 137, no. 10, pp. 1343–1350, 2001.
- [19] H. Kittler, H. Pehamberger, K. Wolff, and M. Binder, "Diagnostic accuracy of dermoscopy", *The lancet oncology*, vol. 3, no. 3, pp. 159–165, 2002.
- [20] D. Piccolo, A. Ferrari, K. Peris, R. Daidone, B. Ruggeri, and S. Chimenti, "Dermoscopic diagnosis by a trained clinician vs. a clinician with minimal dermoscopy training vs. computer-aided diagnosis of 341 pigmented skin lesions: A comparative study", *British Journal of Dermatology*, vol. 147, no. 3, pp. 481–486, 2002.
- [21] A. Blum, H. Luedtke, U. Ellwanger, R. Schwabe, G. Rassner, and C. Garbe, "Digital image analysis for diagnosis of cutaneous melanoma. development of highly effective computer algorithm based on analysis of 837 melanocytic lesions", *British Journal of Dermatology*, vol. 151, no. 5, pp. 1029–1038, 2004.
- [22] A. Ignazio Stanganelli, L. Calori, R. Gori, et al., "Computer aided diagnosis of melanocytic tumors", *Anticancer research*, vol. 25, pp. 4577–4582, 2005.
- [23] J. Lin, H. Koga, M. Takata, and T. Saida, "Dermoscopy of pigmented lesions on mucocutaneous junction and mucous membrane", *British Journal of Dermatology*, vol. 161, no. 6, pp. 1255–1261, 2009.
- [24] V. Noronha, U. Tsomo, A. Jamshed, M. Hai, S. Wategama, R. Baral, M. Piya, and K. Prabhaskar, "A fresh look at oncology facts on south central asia and saarc countries", *South Asian journal of cancer*, vol. 1, no. 1, p. 1, 2012.
- [25] M. A. Sheha, M. S. Mabrouk, A. Sharawy, et al., "Automatic detection of melanoma skin cancer using texture analysis", *International Journal of Computer Applications*, vol. 42, no. 20, pp. 22–26, 2012.